



## Study on the Effect of Laser Welding Parameters on the Microstructure and Mechanical Properties of Ultrafine Grained 304L Stainless Steel

Reihane Nafar Dehsorkhi<sup>1</sup>, Soheil Sabooni<sup>1</sup>, Abdoulmajid Eslami<sup>1</sup>, Fathallah Karimzadeh<sup>1</sup>, Behzad Sadeghian<sup>1</sup>

<sup>1</sup>Department of Materials Engineering, Isfahan University of Technology, Isfahan, 84156-83111, Iran.

Received: 24 April 2016; Accepted: 1 November 2016

Corresponding author email: [r.nafar@ma.iut.ac.ir](mailto:r.nafar@ma.iut.ac.ir)

### ABSTRACT

In the present study, an ultrafine grained (UFG) 304L stainless steel with the average grain size of 300 nm was produced by a combination of cold rolling and annealing. Weldability of the UFG sample was studied by Nd: YAG laser welding under different welding conditions. Taguchi experimental design was used to optimize the effect of frequency, welding time, laser current and laser pulse duration on the resultant microstructure and mechanical properties. X-ray Diffraction (XRD), Optical Microscope (OM), Scanning Electron Microscope (SEM), Transmission Electron Microscope (TEM), microhardness measurements and tension tests were conducted to characterize the sample after thermomechanical processing and laser welding. The results showed that the ultrafine grained steel had the yield strength of 1000 Mpa and the total elongation of 48%, which were almost three times higher than those of the as-received sample. The microstructure of the weld zone was shown to be a mixture of austenite and delta ferrite. The microhardness of the optimized welded sample (315 HV<sub>0.5</sub>) was found to be close to the UFG base metal (350 HV). It was also observed that the hardness of the heat affected zone (HAZ) was lower than that of the weld zone, which was related to the HAZ grain growth during laser welding. The results of optimization also showed that the welding time was the most important parameter affecting the weld strength. Overall, the study showed that laser welding could be an appropriate and alternative welding technique for the joining of UFG steels.

**Keywords:** 304 stainless steel; Ultrafine grain; Laser welding; Taguchi experimental design.

How to cite this article:

Nafar Dehsorkhi R, Karimzadeh F, Sabooni S, Behjati P. Study on the Effect of Laser Welding Parameters on the Microstructure and Mechanical Properties of Ultrafine Grained 304L Stainless Steel. *J Ultrafine Grained Nanostruct Mater*, 2016; 49(2):120-127.

DOI: [10.7508/jufgns.m.2016.02.10](https://doi.org/10.7508/jufgns.m.2016.02.10)

### 1. Introduction

Austenitic stainless steels, particularly AISI 304L, are well known because of the good corrosion resistance and formability. They can be successfully used from cryogenic to high temperature applications, as in furnaces and jet

engines. However, their low strength, particularly in the annealed state, has alleviated their application in some cases [1-2]. Nowadays, several strengthening methods are conventionally applied in metal processing to improve the mechanical properties. These methods include solid solution

strengthening, strengthening by introducing second phase, precipitation hardening and grain refinement [3]. Out of these, grain refinement has been considered as the most effective method, owing to its unique advantage of increasing strength without toughness drop [4]. Most of the published researches conducted on the UFG austenitic stainless steels has focused on their production and mechanical property characterization [5-7]. Weldability, as one of the most important factors determining the applicability of structural UFG materials, has not been systematically investigated. In the case of the fusion welding of UFG steels, considerable grain growth in the heat affected zone (HAZ), and the coarse cast structure in the weld zone are two significant phenomena that can jeopardize the mechanical properties of the welded material, relative to the UFG base material [8]. It seems that among fusion welding techniques, laser welding can be an effective way to join UFG materials due to the lower heat input and the high energy density beam. Another advantage of laser welding over other processes include elimination of flux, narrow width, deep penetration, low residual stress and small distortion [9-10]. Therefore, the aim of the present work was to study the weldability of the UFG 304L stainless steel by laser welding technique and compare the microstructure and mechanical properties of the weld zone with those of the base metal.

**2. Materials and Methods**

The chemical composition of the as-received

304L stainless steel is shown in Table 1. The steel was received in the annealed condition and sheet form with the thickness of 10 mm. Cold rolling was performed to a reduction of 93% at -15 °C, with inter pass cooling. 93% cold rolled samples were then annealed at 700 °C for 2h in order to obtain the UFG austenite structure by martensite to austenite reversion mechanism.

Several specimens with the dimension of 100 40 0.7 mm were cut from the UFG sample and subjected to laser welding using Nd:YAG laser welding machine (IQLB), with the maximum power of 750 W and under Argon shielding gas. The effects of laser welding parameters (welding time, laser frequency, laser pulse duration and laser current) were analyzed systematically using the Taguchi experimental design method with the L9 orthogonal array. In this array, four 3-level factors could be optimized. It should be noted that all experiments were carried out three times and the average data was reported. Table 2 Shows the Taguchi design of experiment used to optimize the welding parameters. Fig. 1 shows a schematic view of the optimized laser welded specimen. No obvious defects, such as lack of fusion/lack of penetration, were observed in this sample.

For cross sectional examinations, samples were cut using a slow-speed saw and mounted in epoxy using the cold-mount equipment. Subsequently, the samples were mechanically ground and polished using papers down to 2400-grit, and this was followed by Al<sub>2</sub>O<sub>3</sub> slurry. Electrolytic etching was performed at 1–2 V for about 10 sec

Table 1- Chemical composition of the AISI 304L stainless steel used in this work

element	C	Cr	Ni	Mo	Mn	Si	P	S	Co	Cu	V	Fe
Wt.%	0.026	18.35	8.01	0.15	1.24	0.323	0.024	0.005	0.129	0.24	0.1	Remain

Table 2- Taguchi design of experiments in the present investigation

Experiment/parameters	Frequency(Hz)	Current(A)	Welding time (sec)	Pulse duration(ms)
S1	55	150	20	3
S2	55	155	25	3.5
S3	55	160	30	4
S4	60	150	25	4
S5	60	155	30	3
S6	60	160	20	3.5
S7	65	150	30	3.5
S8	65	155	20	4
S9	65	160	25	3

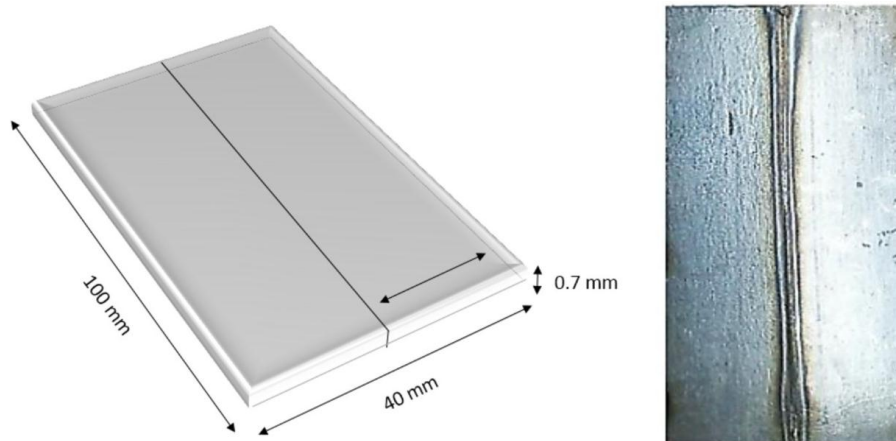


Fig. 1- Schematic view of the laser welded samples.

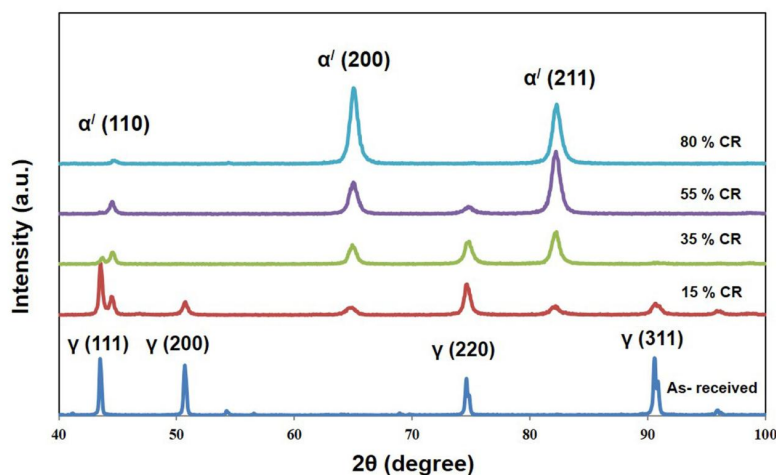


Fig. 2- XRD patterns of as-received and cold rolled samples.

in a solution mixture of 65 ml nitric acid and 35 ml distilled water to reveal the austenite grain boundaries. XRD (Philips, X'PERT-MPD), OM (NIKON-EPIPHOTO300), SEM (Philips, XL-30) and TEM (FEI technai G 2 20 scanning TEM) were employed to evaluate the microstructure after rolling and welding processes. The average grain size was measured using TS-View image analysis software. Microhardness measurements were also performed using a KOOPA-MH3 microhardness tester with a Vickers indenter at the load of 500 gf. Room temperature uniaxial tension tests were also performed according to ASTM E8M with a tensile machine (Hounsfield H50ks) with the crosshead speed of 1mm/min.

### 3. Results and Discussions

#### 3.1. Thermomechanical processing

Fig. 2 shows the XRD patterns of as-received and

cold rolled samples after different reductions. As can be seen, the microstructure of the as-received 304L stainless steel was fully austenitic, consisting only  $\gamma$  (111),  $\gamma$  (200),  $\gamma$  (220) and  $\gamma$  (311) peaks. By increasing the rolling reduction, the intensity of the austenite peak was decreased and the microstructure was gradually transformed to the martensitic state. Fig. 3 shows the TEM micrograph of the 60% cold rolled sample. Martensite lathes could be clearly observed in the microstructure. The average martensite lathes width was found to be around 100 nm at this stage. Only  $\alpha'$  peaks consisting  $\alpha'$  (110),  $\alpha'$  (200) and  $\alpha'$  (211) were visible after 80% rolling reduction. Therefore, it could be concluded that martensitic transformation fully occurred and the sample was ready for the annealing process.

93% cold rolled samples were then annealed at 700 °C for 2h to obtain austenitic structure thorough martensite to austenite reversion. Fig.

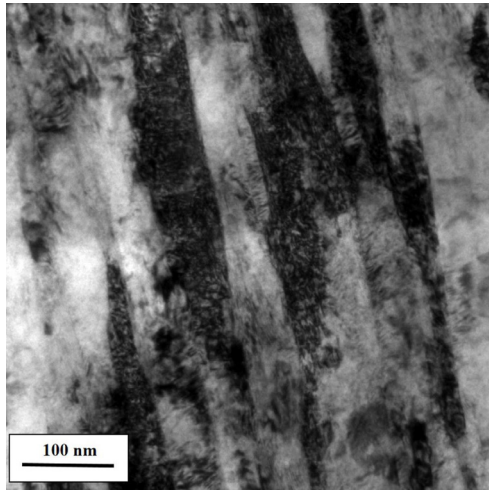


Fig. 3- TEM micrograph of the 60% rolled sample showing nanometric martensite lathes.

4(a) and Fig. 4(b) show the SEM micrographs of the as-received and UFG sample, respectively. As can be seen, the average grain size was reduced from 30  $\mu\text{m}$  in the as-received sample to around 300 nm after thermomechanical processing. It should be noted that the elongated phase in the SEM images was related to the intergranular delta phase existing in the initial microstructure that

was not affected by the rolling process. Grain refinement to nanometric scales caused yield stress increase. The yield stress of the UFG sample was increased to about 1000 Mpa, which was about three times higher than that for the as-received sample (Fig. 4(c)). Beside the high strength, the UFG steel showed 48% elongation ( $\Delta L/L_0$ ), which was comparable to that of the as-received sample.

### 3.2. Welding

Laser welding was applied to the UFG samples to study the effect of welding parameters on the microstructure and the mechanical properties of the UFG 304L stainless steel. Table 3 shows the weldments characteristics included weld zone and HAZ austenite grain size, ferrite percentage in the weld zone and the weldments mechanical properties. Sample 3 shows the yield stress of 567 Mpa and the ultimate tensile strength (UTS) of 803 Mpa, which were considerably higher than those of other samples. The weld zone austenite grain size for this sample was about 4.7  $\mu\text{m}$ , which was lower than that of the others.

The microstructure of the weld zone and HAZ of the sample 3 is shown in Fig. 5. It should be noted that full penetration was achieved in the weld zone.

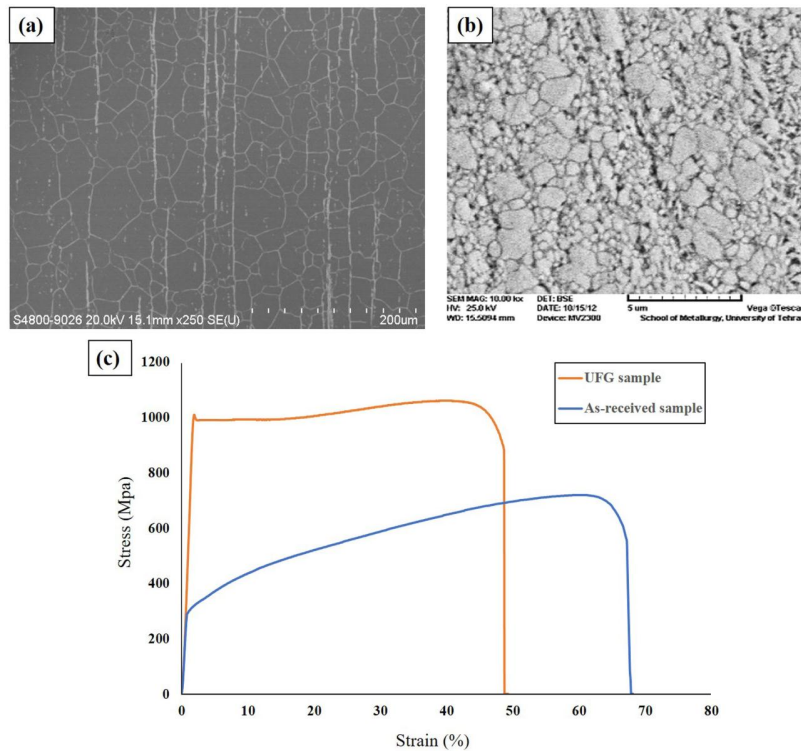


Fig. 4- SEM Micrographs of the as-received (a) and UFG (b) samples along with their stress – strain curve (c).

As can be seen, the weld zone contained austenite and a low amount of  $\delta$ -ferrite (12%). Epitaxial growth could also be clearly seen at the weld zone / HAZ interface. The XRD pattern of the weld zone (Fig. 6) confirmed the results of microstructural studies, showing that the weld zone was composed of austenite and  $\delta$ -ferrite. As can be evaluated by the XRD pattern, the amount of austenite phase in the weld zone was higher than that of  $\delta$ -ferrite. It is well known that the solidification type and the microstructure of weld zone in the fusion welding of austenitic stainless steels strongly depends on the

$Cr_{eq}/Ni_{eq}$  [11]. It is also accepted that by increasing the amount of  $Cr_{eq}/Ni_{eq}$ , the primary solidification phase is changed from austenite to delta ferrite [11-12]. In the normal cooling rates (for example, in Gas-Tungsten Arc Welding), this change normally occurs at  $Cr_{eq}/Ni_{eq} = 1.5$ . Meanwhile, the welding speed can considerably influence the changing ratio, as it normally occurs at the  $Cr_{eq}/Ni_{eq}$  of about 1.8 or more in the laser welding. That was why the microstructure of the welded sample mostly contained the austenite phase.

Fig. 7 shows the microhardness profile along the

Table 3- Weld zone and HAZ austenite grain size, ferrite percentage in the weld zone and weldments mechanical properties

sample	Weld zone austenite grain size ( $\mu\text{m}$ )	HAZ austenite grain size ( $\mu\text{m}$ )	Ferrite percentage in the weld zone (%)	Yield stress (Mpa)	Ultimate tensile strength (Mpa)	Elongation (%)
S1	$10.5 \pm 0.5$	$15.7 \pm 1.2$	7	308	391	3
S2	$7.1 \pm 0.3$	$10.9 \pm 0.7$	10	230	291	3
S3	$4.7 \pm 0.5$	$5.3 \pm 0.4$	12	567	803	6.5
S4	$8.5 \pm 0.4$	$10.9 \pm 0.7$	7	305	482	7.6
S5	$5.1 \pm 0.2$	$9.6 \pm 0.6$	3	321	521	6
S6	$5.5 \pm 0.2$	$8.6 \pm 0.5$	8	290	544	7
S7	$5.9 \pm 0.4$	$13.2 \pm 1.0$	5	313	506	7
S8	$3.4 \pm 0.3$	$7.4 \pm 0.5$	2	350	455	11.5
S9	$5.6 \pm 0.4$	$8.6 \pm 0.5$	13	226	387	3

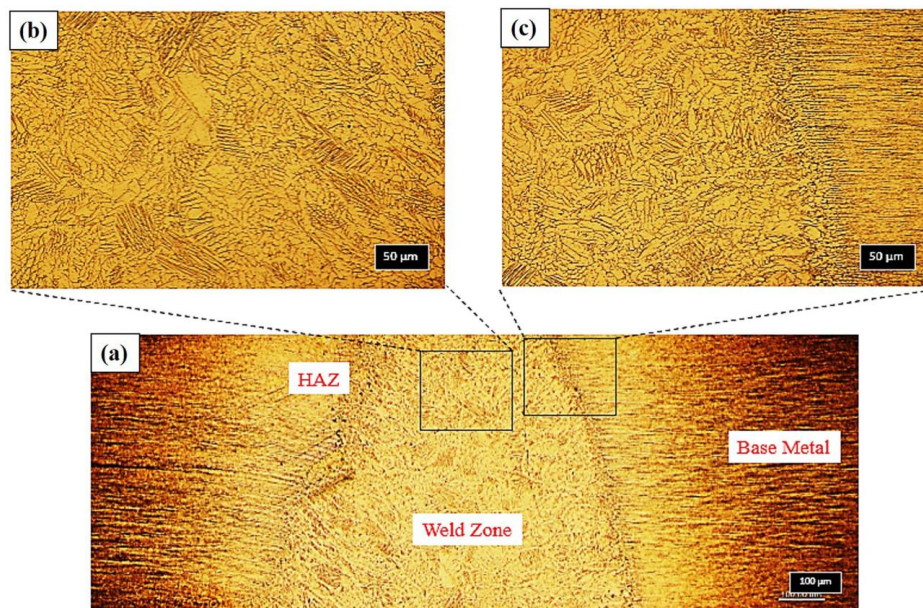


Fig. 5- a) low magnification micrograph of the weld zone and HAZ of the sample 3, b) The microstructure of the weld zone with higher magnification, and c) The weld zone and HAZ interface with higher magnification.

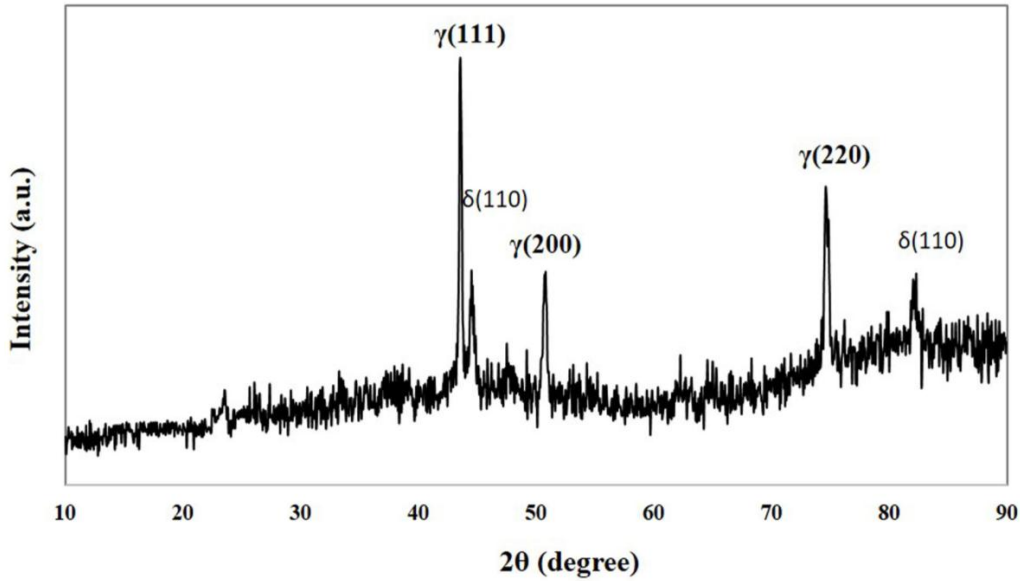


Fig. 6- The XRD pattern of the sample 3 weld zone.

transverse direction of the sample 3 cross section. It should be noted that the average hardness of the weld zone was 315 HV<sub>0.5kg</sub>, which was very close to the base metal (350 HV<sub>0.5kg</sub>). As can be seen, the width of the weld zone and HAZ was very narrow, which could be regarded as one of the most important advantages of the laser welding process. It is worth noting that the hardness of HAZ was lower than that of the weld zone. Based on Table 2, the average austenite grain size in the weld zone and HAZ of sample 3 was around 4.7 μm and 5.3

μm. Therefore, the small difference in the hardness could be related to the higher austenite grain size of the weld zone rather than HAZ.

In the present study, the optimum welding condition was selected based on signal to noise ratio (S/N ratio) from the experimental results. S/N ratio was calculated using the following equation:

$$S/N_i = 10 \log \frac{\bar{y}_i^2}{s_i^2} \quad (\text{eq. 1})$$

Where  $\bar{Y}_i$  and  $S_i^2$  can be calculated by equations

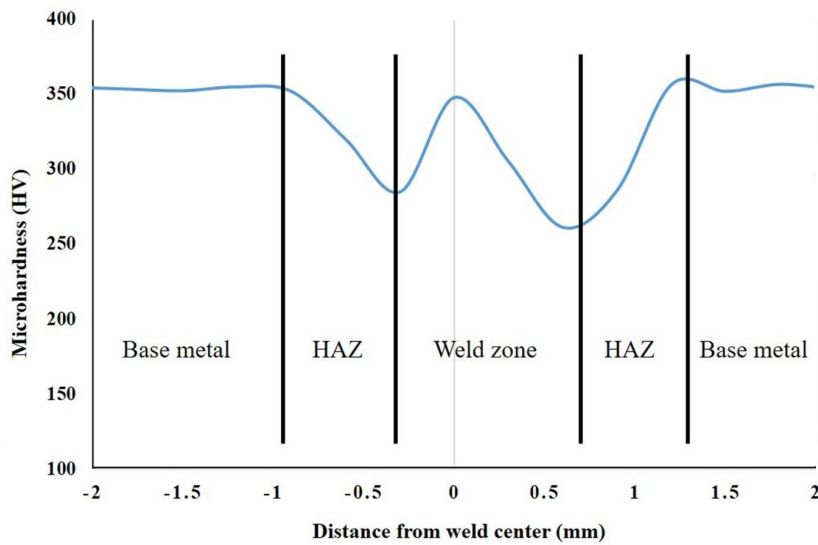


Fig. 7- Microhardness profile along the transverse direction of the sample 3.

(2) and (3), respectively.

$$\bar{y}_i = \frac{1}{N_i} \sum_{u=1}^{N_i} y_{i.u} \quad (\text{eq. 2})$$

$$s_i^2 = \frac{1}{N_i - 1} \sum_{u=1}^{N_i} (y_{i.u} - \bar{y}_i)^2 \quad (\text{eq. 3})$$

$i$  is the number of experiments and  $N_i$  is the number of covered experiments, which could be considered as 9 and 81 in the present investigation. There are three S/N ratios of common interest for the optimization of static problem, i.e., the larger is better, the lower is better and the nominal is better. In the present study, the weld zone strength was used as the characteristic to be optimized. Since the weld zone strength was intended to be maximized, (the larger is better) situation was selected. The S/N ratio has been plotted against the laser welding parameters in Fig. 8. As can be seen, the weld zone strength was affected by all parameters. Also, the welding time is known as the most effective parameter determining the weld strength. Based on the S/N analysis, the following parameters (welding frequency: 60 Hz, welding current: 160 A, welding time: 30 sec and pulse duration: 4 ms) were identified as the optimized condition for laser welding of UFG 304L stainless steel which is very close to the parameters used for the sample 3.

**4. Conclusions**

An ultrafine grained 304L stainless steel with the average grain size of 300 nm was produced by

a combination of cold rolling and annealing. The yield strength of 1000 Mpa and the total elongation of 48% were achieved. The yield strength was determined to be about three times higher than that of the as-received sample. Laser welding was successfully applied to the UFG sample. Taguchi experimental design was used to optimize the effect of frequency, laser current, laser pulse duration and welding time on the resultant microstructure and the mechanical properties. The results showed that the microstructure of the weld zone consisted of austenite and delta ferrite, without any defects. Microhardness measurement also showed that the weld zone microhardness (315 HV<sub>0.5</sub>) was very close to the base metal microhardness (350 HV<sub>0.5</sub>), confirming the high welding efficiency. It was observed that the microhardness and efficiency of the welding process were enhanced by increasing the welding current and reduction of frequency. Overall, the results of the present study revealed that that laser welding could be an appropriate welding technique for the joining of UFG steels.

**References**

1. Davis J. ASM Specialty Handbook–Stainless Steels. Materials Park, USA, ASM International. 1994.
2. Lo KH, Shek CH, Lai JK. Recent developments in stainless steels. Materials Science and Engineering: R: Reports. 2009;65(4):39-104.
3. Karjalainen LP, Taulavuori T, Sellman M, Kyrolainen A. Some strengthening methods for austenitic stainless steels. Steel Research International. 2008;79(6):404.
4. Song R, Ponge D, Raabe D, Speer JG, Matlock DK. Overview of processing, microstructure and mechanical properties of ultrafine grained bcc steels. Materials Science and

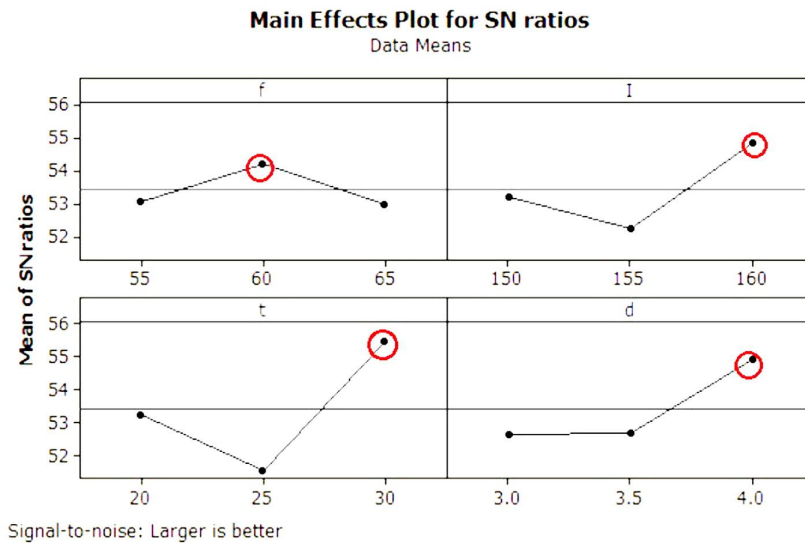


Fig. 8- The effect of laser welding parameters on the S/N ratio.

- Engineering: A. 2006;441(1):1-7.
5. Sabooni S, Karimzadeh F, Enayati MH, Ngan AH. The role of martensitic transformation on bimodal grain structure in ultrafine grained AISI 304L stainless steel. *Materials Science and Engineering: A*. 2015;636:221-30.
  6. Rezaee A, Kermanpur A, Najafizadeh A, Moallemi M, Baghbadorani HS. Investigation of cold rolling variables on the formation of strain-induced martensite in 201L stainless steel. *Materials & Design*. 2013;46:49-53.
  7. Momeni A, Abbasi SM. Repetitive thermomechanical processing towards ultrafine grain structure in 301, 304 and 304L stainless steels. *Journal of Materials Science & Technology*. 2011;27(4):338-43.
  8. Weng Y, editor. *Ultra-fine grained steels*. Springer Science & Business Media; 2009.
  9. Mazumder J. Laser welding: state of the art review. *Journal of the Minerals, Metals & Materials Society*. 1982;34(7):16-24.
  10. Mackwood AP, Crafer RC. Thermal modelling of laser welding and related processes: a literature review. *Optics & Laser Technology*. 2005;37(2):99-115.
  11. Lippold JC. Solidification behavior and cracking susceptibility of pulsed-laser welds in austenitic stainless steels. *Welding Journal Including Welding Research Supplement*. 1994;73(6):129-139.
  12. Guo W, Kar A. Prediction of microstructures in laser welding of stainless steel AISI 304. *Journal of Laser Applications*. 1999;11(4):185-9.